18

Study on Thixotropic Plastic Forming of Wrought Magnesium Alloy

Hong Yan
Nanchang University
China

1. Introduction

Semi-sold material (SSM) forming was proposed by Flemings et al. from Massachusetts Institute of Technology (MIT) in 1972. SSM forming is one of the near-net-shape-forming processes which manufacture the final part by loading the materials at a temperature between liquidus and solidus. This way of forming difficult-to-machine materials is useful because there is much less strain resistance compared with conventional forging processes. Furthermore, energy savings and compact forming machinery become possible because of forming at smaller loads. Therefore, SSM forming is taken for one of the near-net-shape-forming having the best future in the 21th century (Kang et al., 1999).

Compared with casting magnesium alloys, wrought magnesium alloys have higher mechanical strength, better ductility and more varied mechanical properties. But the magnesium element is so lively that it is liable to be oxidated or burned during smelting and working. Simultaneously, the lower strength under high temperature and creep properties restrict the application of magnesium alloys in high temperature occasion. In addition, influenced by the microstructure, magnesium alloys have low deforming property and poor plasticity. Start from pursuing to the net forming technology and lighter production, the semi-solid thixo-forming technology becomes a preferred hot forming technique for wrought magnesium alloys (Flemings, 1991; Yan & Xia, 2005).

At high solid volume fraction (≥50%~60%), the behaviour of semi-solid material mechanics in the thixotropic plastic deformation process can be solved only when the relationship between stress and strain is obtained. Recently there have been a lot of studies on this field. A stress-strain relationship was investigated through considering the separate coefficient for semi-solid materials (Kang et al., 1998). The mathematical models of yield criterion and constitutive equations of mushy/semi-solid alloys were proposed (Kiuchi et al., 1998). The viscoplastic constitutive equations of SSM were presented by analyzing viscoplastic behaviour of material (Martin et al., 1997). On the basis of analysis of the thixotropic plastic deformation behaviour of semi-solid wrought magnesium alloy in compression process (Yan & Zhou, 2006), its constitutive model was established (Yan & Zhou, 2006).

Semi-solid processing technology is a new metal working technology in recent years, in which the alloys in semi-solid state have the excellent thixotropic and rheological properties. The deformation resistance in semi-solid state is influenced by not only solid volume

fraction and shear rate but also time, it's difficult to simulate semi-solid metal processing. Many researchers had carried out many investigations to simulations of semi-solid metal processing. The filling behaviours of semi-solid materials were described by computer simulation (Tims et al., 1996). Three-dimensional filling analyses with considering flow phenomena and solidification as a function of viscosity were performed (Lipinski & Flender, 1998). The numerical simulations on thixotropic as well as rheological forming focused mainly on the treatment of slurry or description of flow filling process. The few numerical simulations on the thixotropic forge in high solid volume fraction were reported.

The three main procedures in semi-solid metal processing are blank-making (Yan et al., 2005), reheating (Yan et al., 2006) and thixoforming (Yan et al., 2008). Thixo-forming is the last procedure, which benefits the quality of workpiece. Therefore the technological parameters in wrought magnesium alloy thixoforming process are well understood, analyzed, controlled and optimized using numerical simulation and experimental methods.

2. Thixotropic deformation behaviours of wrought magnesium alloy

2.1 Expermental

The experimental materials were the semi-solid wrought magnesium alloy (AZ61) and the conventional as-casted. In this study the chemical compositions of AZ61 magnesium alloy were listed in Table 1.

Element	Al	Mn	Zn	Si	Cu	Ni	Fe	others	Mg
Weight(%)	5.8%～7.2%	>0.15%	0.40%～1.5%	0.10%	0.05%	0.05%	0.005%	0.30%	Balance

Table 1. Chemical compositions of AZ61 magnesium alloy used in the experiment

The experiments were carried out in the Gleeble-1500 dynamic material testing machine. The sample was heated with the electric resistance method, whose temperature was measured by thermocouples. The graphite slices were placed between the specimen and the compression heads for reducing the influence of friction on experiment.

The solidus of AZ61 magnesium alloy was 525^{o}C, the liquidus was 620^{o}C. Therefore, the semi-solid deformation temperature period was 525^{o}C -620^{o}C. In order to study and master the characteristics of semi-solid magnesium alloy mechanics at high solid volume fraction, the deformation temperatures were taken as 528^{o}C, 538^{o}C, 550^{o}C and 560^{o}C respectively. According to the heating procedure shown in Fig.1, the initial heating rate was 10^{o}C/s; when the sample's temperature reached 500^{o}C, the temperature rate was down to 1^{o}C/s. The above scheduled temperatures reached with holding time 10mins. Then the semi-solid compression experiments were done under the strain rates of 0.1s^{-1}, 0.5s^{-1}, 5s^{-1} and 10s^{-1} respectively, in which the total strain was 0.8. At the same time, the compression of as-casted specimen was carried out with its temperature heated 522^{o}C and strain rate $\dot{\varepsilon} = 0.1s^{-1}$. The sample was taken immediately out for water quenching. Then the specimen was made to metallurgical phase sample and corrupted with 4% nitric and liquor, its microstructure changes were observed under the optical microscope.

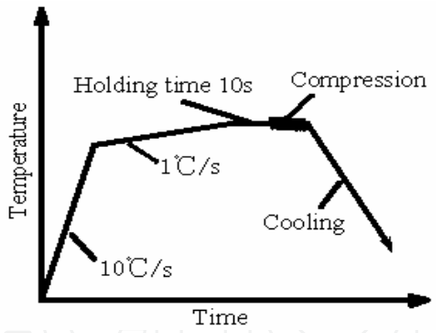

Fig. 1. Experimental heating procedure

2.2 The deformed and undeformed microstructures of wrought magnesium alloy

The undeformed microstructure of AZ61 magnesium alloy was composed of the branched grains that had a few large branched grains shown in Fig.2a. An ideal semisolid non-branched grain microstructure was obtained with prior compressive deformation 22%, heat treatment temperature 595°C and holding time 40min (Fig.2b) (Yan et al., 2005). Then the deformed microstructure of semi-solid AZ61 alloy was gained in thixotropic compression process.

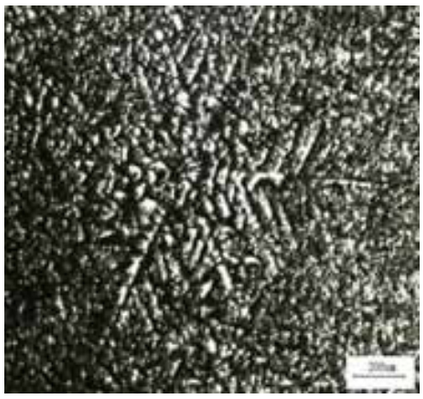

(a) Microstructure of conventional as-casted

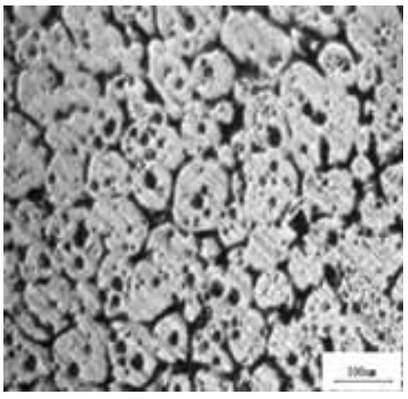

(b) Microstructure of semi-solid sample

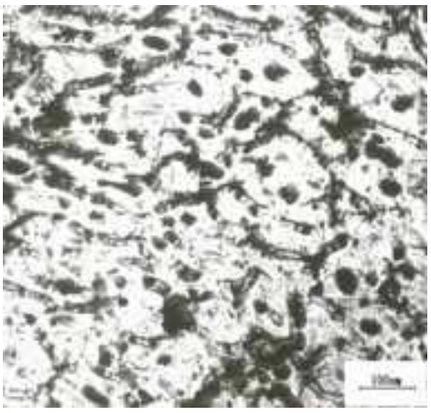

(c) Thixotropic deformed microstructure at free deformation zone

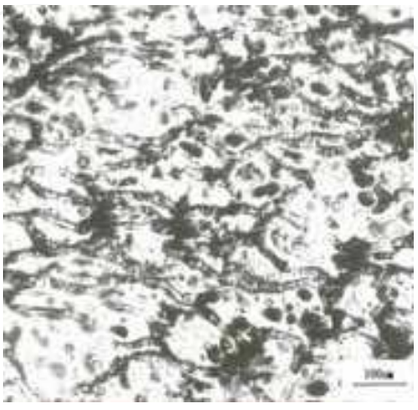

(d) Thixotropic deformed microstructure at large deformation zone

Fig. 2. The undeformed and deformed microstructures of AZ61 magnesium alloy

After the semi-solid AZ61 alloy was pressed by the large plastic deformation, its structure was changed obviously. The regular globular grains were flatted, having the unregular shape. Few liquid phases in the semi-solid material run basically off, the eutectic phase was deformed accordingly. As shown in Fig.2c, Fig.2d, the deformation degree of semi-solid globular grains was associated with the position of deformation zone in sample. The deformation degree in the centre zone (large deformation zone) was larger than one in brim zone (free deformation zone). In the whole thixotropic compression deformation process of semi-solid AZ61 magnesium alloy, the four deformation mechanisms exist such as liquid/flow; flow of liquid incorporating solid particles; sliding between solid particles and plastic deformation of solid particles mechanisms. Because of high solid volume fraction in the thixotropic compression deformation process, the sliding between solid particles and plastic deformation of solid particles mechanisms dominated in the centre of sample, the mix mechanisms ruled in the brim.

2.3 The relationships between stress and strain in thixotropic compression processes

The true stress-strain curves of thixotropic compression at the different temperatures for strain rate $\dot{\varepsilon} = 5s^{-1}$ were shown in Fig.3a, whose developing trends resembled basically. At the beginning of compression deformation, the strain value increased from 0 to 0.1. The stress increased rapidly with the strain increasing. When the stress reached the peak value, its strain value was around 0.1. After the stress reached up peak value, the stress held a little time with the strain increasing, the skeleton composed by solid particle slid and deformed gradually until it was destroyed thoroughly under pressure. When the stress peak value platform was passed, the stress descended slowly with the strain increasing, the softening phenomenon took place. As shown in Fig.3a, the stress peak values at temperatures of 550^{o}C, 538^{o}C and 522^{o}C were 20.60MPa, 26.4MPa and 37.63MPa respectively. When the semi-solid temperature decreased from 550^{o}C to 538^{o}C, the stress peak value increased 5.81MPa, its growth rate was 25%. However, when the semi-solid temperature decreased from 538^{o}C to 522^{o}C, the stress peak value increased 11.22MPa, its growth rate was 43%. It was shown hat the deformation resistance of semi-solid AZ61 magnesium alloy was obviously smaller than one of conventional as-casted sample.

As shown in the Fig.3a and Fig.3b, under the same strain rate condition, the higher deformation temperature, the lower deformation resistance, and deformation resistance decreased obviously with the deformation temperature increasing. This was because the higher deformation temperature, the thicker thin film of liquid phase in grain boundary, and then the grain shape neared to spheroid, which made it slip and turn easily, the deformation resistance decreased. In the thixotropic compression deformation process of semi-solid AZ61 magnesium alloy, the deformed mechanisms were four major mechanisms: liquid/flow; flow of liquid incorporating solid particles; sliding between solid particles and plastic deformation of solid particles mechanisms.

However, which deformed mechanism was predominant? The increase or decrease of deformation resistance was decided by the solid volume fraction. When the solid volume fraction was lower, the solid particles were surrounded by liquid phase, and the deformation took place with liquid flow. The deformation force was thus very small, which was only required to overcome liquid resistance. When the solid volume fraction was higher, the liquid was few, the solid particles contacted with each other. The deformation force was required to overcome the friction generated from the sliding between solid

particles, and also to overcome the restriction of the solid particle movement due to the spatial constraint imposed by the surrounding particles. Therefore, in the beginning of compression process, the liquid/flow mechanism is unimportant, the other three mechanisms (namely flow of liquid incorporating solid particles, sliding between solid particles and plastic deformation of solid particles) are dominant. The original stress value was large, because the solid particles contacted with each other in very short time, taking place plastic deformation and finally leading the true stress rapidly increasing. At the same time, the higher the strain rate, the smaller the function of liquid/flow and flow of liquid

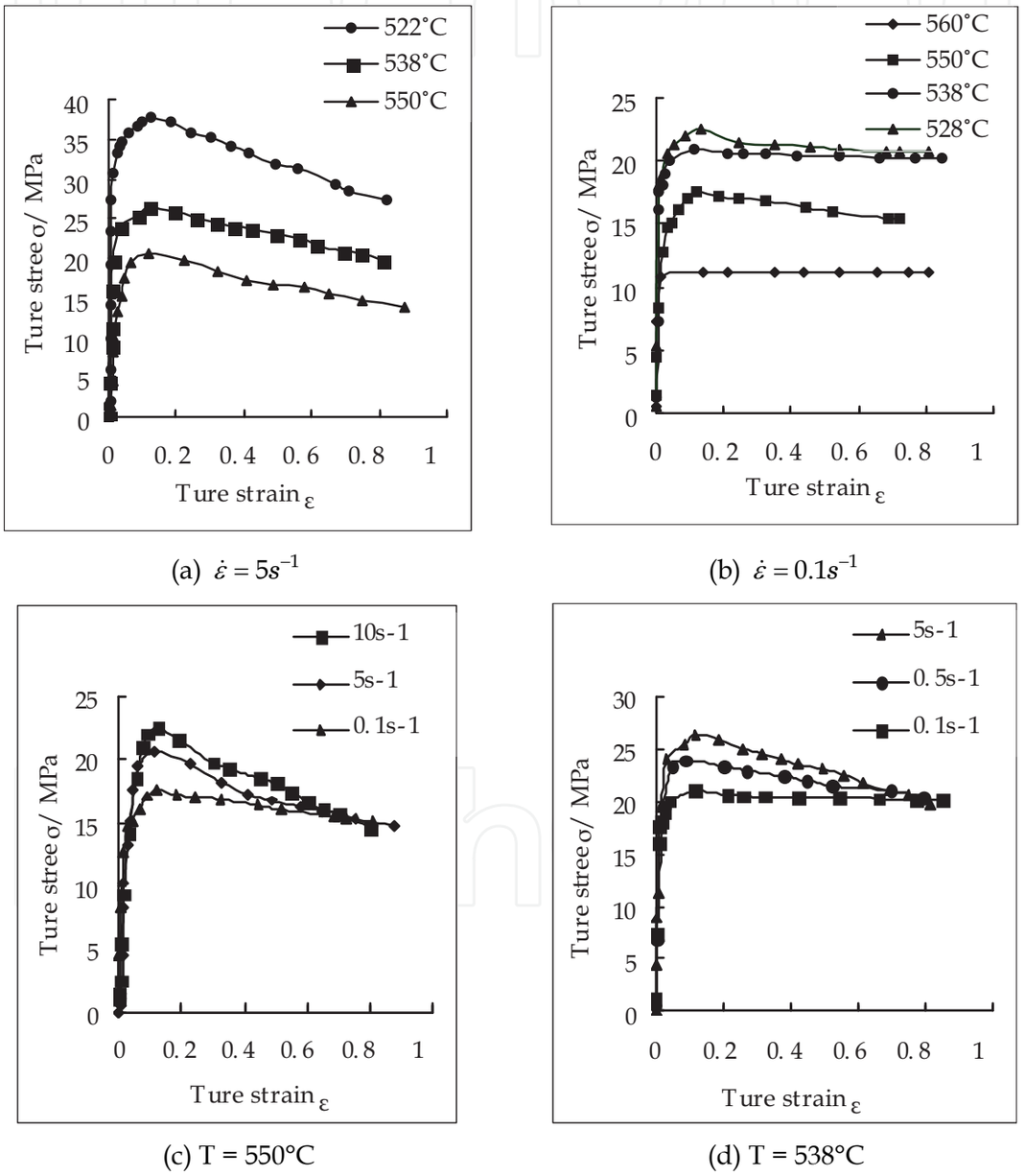

(a) $\dot{\varepsilon} = 5s^{-1}$ (b) $\dot{\varepsilon} = 0.1s^{-1}$

(c) T = 550°C (d) T = 538°C

Fig. 3. Relationships between true strain and stress in thixotropic compression deformation process

incorporating solid particles mechanisms in the same deformation temperature, in which the sliding between solid particles and the plastic deformation of solid particles mechanisms were dominant. The corresponding stress was larger.

3. Constitutive model of thixotropic plastic forming

3.1 Establishment of constitutive model

The relationship among processing parameters (strain rate, strain, temperature, liquid volume fraction) and stress was studied for semi-solid material at high solid volume fraction (Yan & Xia, 2002; Yan & Zhou, 2006). The relationship among variables was nonlinear. The relationship among stress σ, strain rate $\dot{\varepsilon}_z$ and strain ε_z was power function. The relationship among stress σ, temperature T and liquid volume fraction f_L was exponential function. So the relationship among stress σ, strain rate $\dot{\varepsilon}_z$, strain ε_z, temperature T and liquid volume fraction f_L was supposed as follows:

$$\sigma = \alpha_0 \cdot \exp(\alpha_1 T) \cdot \dot{\varepsilon}_z^{\alpha_2} \cdot \varepsilon_z^{\alpha_3} \cdot [1 - \beta f_L]^{\alpha_4} \tag{1}$$

Where σ was stress, ε_z strain, $\dot{\varepsilon}_z$ strain rate, T temperature, β geometric constant (= 1.5), α_0, α_1, α_2, α_3 and α_4 were material constants, f_L liquid fraction. $f_L = (\frac{T_M - T_L}{T_M - T})^{\frac{1}{1-K}}$, T_M the melting point of material, T_L liquidus temperature, k the distribution ratio of equilibrium.

The parameters in proposed constitutive model were determined by the multiple nonlinear regression method. Experimental dates were obtained in the unilateral compression processes. The nonlinear equation was transformed into linear one using logarithms for Eq. (1).

$$\ln\sigma = \ln\alpha_0 + \alpha_1 / T + \alpha_2 \ln\dot{\varepsilon}_z + \alpha_3 \ln\varepsilon_z + \alpha_4 \ln[1 - \beta f_L] \tag{2}$$

Where $y = \ln\sigma$, $A_0 = \ln\alpha_0$, $A_1 = \alpha_1$, $A_2 = \alpha_2$, $A_3 = \alpha_3$, $A_4 = \alpha_4$, $X_1 = 1/T$, $X_2 = \ln\dot{\varepsilon}_z$, $X_3 = \ln\varepsilon_z$, $X_4 = \ln(1 - \beta f_L)$.

Eq. (2) was changed as follow:

$$y = A_0 + A_1 X_1 + A_2 X_2 + A_3 X_3 + A_4 X_4 \tag{3}$$

The regression calculation and analysis of above equation were done by SPSS (Statistical Package for the Social Sciences). The usual statistics values were listed in Table 2 where the correlation coefficient R = 0.951, determination coefficient R^2 = 0.904, adjusted determination coefficient $\bar{R}^2$ =0.899, the Std. Error of the Estimate S=0.071, Durbin-Watson=0.343. Those showed that the representativeness of proposed constitutive model was strong.

R	R^2	$\bar{R}^2$	S	Durbin-Watson
0.951	0.904	0.899	0.07101259	0.343

Table 2. Model Summary

The analysis of variance was listed in Table 3 where the statistics values F=206.805, the concomitant probability value p<0.001. The relationship between independent variable x and dependent variable y was linear. In addition, Sum of Squares regression was 4.167, the residual error sum of squares 0.443, the total sum of squares 4.610, d.f. was degree of freedom.

	Sum of Squares	d. f.	Mean Square	F	Sig.
Regression	4.167	4	1.042	206.805	0.000
Residual	0.443	88	0.005		
Total	4.610	92			

Table 3. ANOVA

The analysis results of regression coefficients were listed in Table 4 where t was the inspection & statistics value of regression coefficient, Sig. was the concomitant probability value. It can be seen that the constant term A_0=25.000; regression coefficients A_1= -11560.385, A_2=0.026, A_3=-0.09, A_4=7.655; the inspection & statistics value of regression coefficient t= 6.443, -5.651, 5.761, -10.671, 8.220; the concomitant probability value p<0.001. Those indicated that the constitutive model had significance meaning.

$$y = 25 - 11560X_{1x} + 0.026X_2 - 0.09X_3 + 7.655X_4 \tag{4}$$

So Esq. (1) became

$$\sigma = \exp(25 - 11560/T) \cdot \dot{\varepsilon}_Z^{0.026} \cdot \varepsilon_Z^{-0.09} \cdot (1 - \beta f_L)^{7.655} \tag{5}$$

Eq.(5) was the nonlinear constitutive relationship of semi-solid AZ61.

	Unstandardized Coefficients		Standardized Coefficients	t	Sig.
	B	Std. error			
A_0	25.000	3.881		6.443	0.000
A_1	-11560.385	2045.703	-1.815	-5.651	0.000
A_2	0.026	0.005	0.217	5.761	0.000
A_3	-0.09	0.012	-0.356	-10.671	0.000
A_4	7.655	0.931	2.618	8.220	0.000

Table 4. Coefficients

3.2 Analytical results and discussion

Comparisons between the predicted and experimental results in thixotropic compression processes were shown in Fig.4 The true stress-strain curves of thixotropic compression at the different temperatures for strain rate $\dot{\varepsilon}_z$ = 0.1s-1 were shown in Fig.4a, whose developing trends resembled basically. At the beginning of compression deformation, the strain value

increased from 0 to 0.1. The stress increased rapidly with the strain increasing. When the stress reached the peak value, its strain value was around 0.1. After the stress reached up peak value, the stress held a little time with the strain increasing, the skeleton composed by solid particle slid and deformed gradually until it was destroyed thoroughly under pressure. When the stress peak value platform was passed, the stress descended slowly with the strain increasing, the softening phenomenon took place. Under the same strain rate condition, the higher the deformation temperature, the lower the deformation resistance, and the deformation resistance decreased obviously with the deformation temperature increasing. The true stress-strain curves of thixotropic plastic compression at the different strain rate under the same deformation temperature were shown in Fig.4b. It is seen that under the same deformation temperature, the lower the strain rate, the lower the deformation resistance and the peak value.

Fig.4 showed that the results calculated by multiple nonlinear regression method were good agreement with experimental ones. So, the proposed constitutive model had the higher forecast precision and practice meaning.

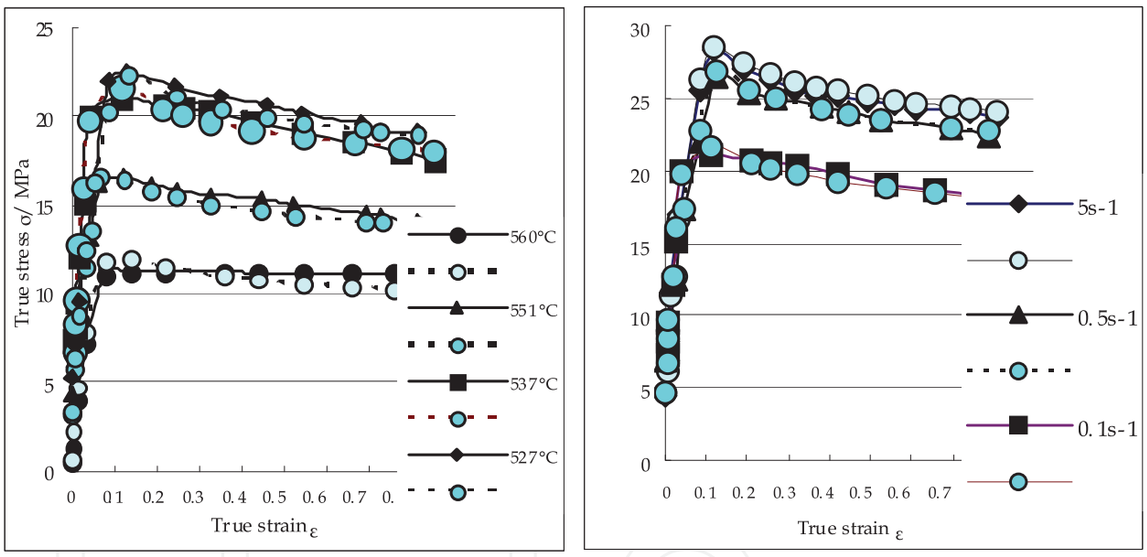

(a) $\dot{\varepsilon} = 0.1s^{-1}$ (b) T = 538°C

Fig. 4. Comparisons between predicted and experimental results in thixotropic plastic compression processes

4. Numerical simulation of thixotropic plastic forming

To investigate thixoforming process with numerical simulation method, which was a nonlinear system, some assumptions were taken as follows: (1) The semi-solid metal was assumed as a continuous and incompressible metal fluid. (2) The solid grains in semi-solid metal were uniformly distributed in liquid phase, and because of the large deformation in forming, the semi-solid material was considered as an isotropy uniform medium.

The material adopted in this paper was AZ61 wrought magnesium alloy, and the simulations were performed in traditional forging/extrusion and thixo-forging/thixo-

extrusion processes. The flow stress model of AZ61 wrought magnesium alloy in traditional forging/extrusion processes was presented as follows (Zhou et al., 2004):

$$\sigma = A_5 \cdot \varepsilon^n \cdot \dot{\varepsilon}^m \cdot \exp(s\varepsilon - \frac{Q}{RT}) \tag{6}$$

Where A_5 is constant; n is exponent; m is strain-rate sensitivity; s is exponent for the strain softening influence, negative; Q is activation energy; R is gas constant (8.31kJ/mol).
The flow stress model of AZ61 wrought magnesium alloy in thixo-forging/thixo-extrusion processes was expressed as follows (Yan & Zhou, 2006)

$$\sigma = \exp(25 - 11560 / T) \cdot \dot{\varepsilon}_Z^{0.026} \cdot \varepsilon_Z^{-0.09} \cdot (1 - \beta f_L)^{7.655} \tag{7}$$

Where σ is the stress; ε_z the strain; $\dot{\varepsilon}_z$ the strain rate; T temperature; β constant; f_L liquid volume fraction.

4.1 Finite element analysis of thixo-forging

In this study, the magnesium alloy workpiece is formed by the close-forge method. The experiment set-up was shown in Fig.5. Fig.6 shows the workpiece, whose structure and flow character are complicated. Comparisons between forging and thixoforming of the workpiece will be done and predicted in advance using numerical simulation. This is an effective method to instruct application of semi-solid forming technology into its practice production. The same simulated parameters are used to analyze the differences of mechanics properties, flow rule and temperature between forging and thixoforming processes. The materials are normal and semi-solid AZ61 magnesium alloy respectively.
Fig.7 shows the load-stroke curves at 559°C in forging and thixoforming. In the two forming processes, the loads in the initial stage varied gently. When the stroke reached 12.3mm, the rest of the load increased evidently, resulted from forming of claw. When the stroke reached

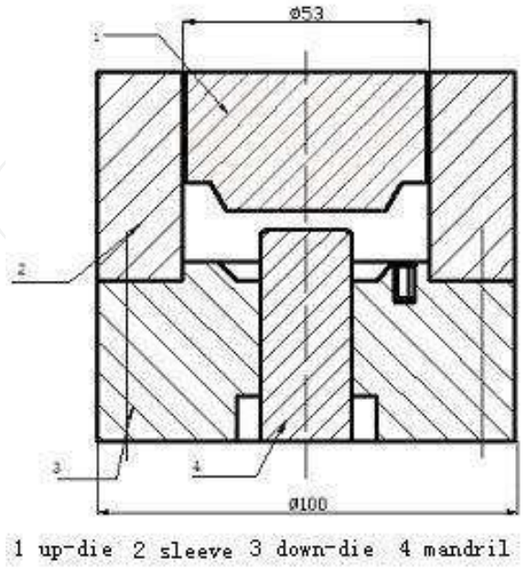

Fig. 5. Experiment set-up

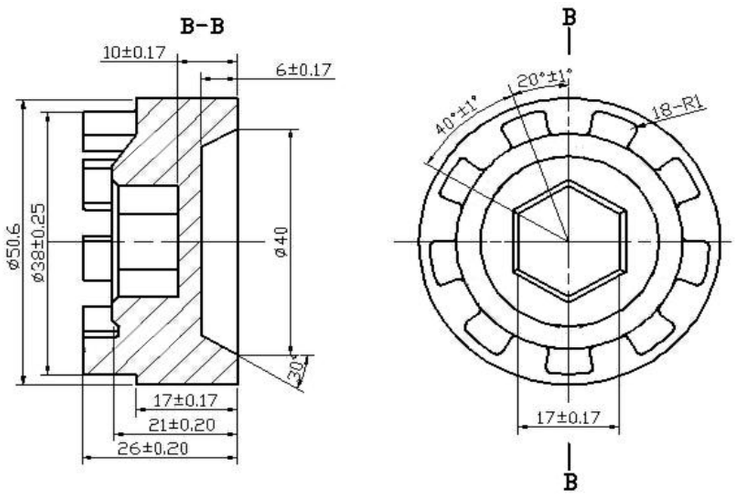

Fig. 6. AZ61 alloy workpiece

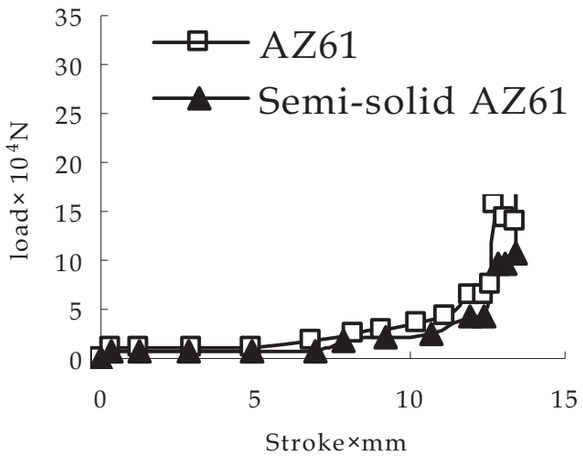

Fig. 7. Load-stroke curve at 559℃

12.8mm, the load had the trend of decreasing. And in the last stage of filling, the load rose sharply. From Fig.7 we can get that at 12.88mm, the load of forging is much larger than that of thixoforming, and it can be illustrated that the deformation resistance in semi-solid forming process was smaller than that in forging process, in which the former filling property was superior to the latter. The maximum simulated load in forging was 0.29MN, The maximum simulated load in thixo-forging was 0.19MN. The results presented that in the same conditions, the deformation resistance in thixo-forging was about 1/3 less than that in forging, which show a very good agreement with those observed in the experiment. But they were less than the experimental results. The friction coefficient was invariability, and interference fit was used in the simulation model, in which the material can't be squeezed into the gap between dies. The workpiece margin was formed in the experiment, which resulted that experimental loads were higher than simulation ones.

Fig.8 showed the effective stress distributions before completed fill in both forging and thixo-forging at 559°C.The effective stress distribution existed unevenly in forging, whose value (the final 92.4Mpa) was so big that the residual stress could be resulted in workpiece.

That needed to add another working procedure for treating. Effective stress distribution in thixoforming was uniform and its value (the final 30.8Mpa) was small, which was contributed from the excellent fluidity of semi-solid metal.

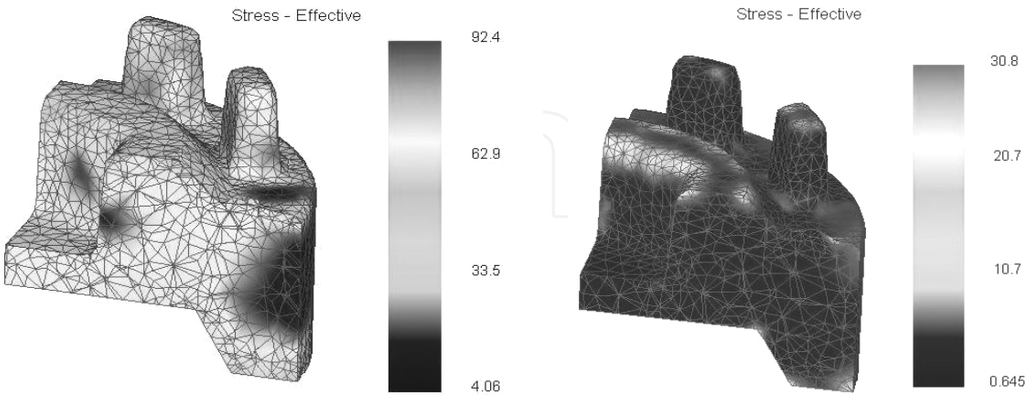

(a) Traditional forging (b) Thixo-forging

Fig. 8. Effective stress distributions of wrought magnesium alloy in traditional forging and thixo-forging processes

Fig.9 and Fig.10 gave the effective strain simulated results in forging and thixo-forging respectively. In the initial stage, the hexagon hole in central section of workpiece was extruded and the rest moved in the rigid motion. In this stage, the strain distributions had few differences between forging and thixo-forging. As the stroke increased, metal deformation entered into the second stage, in which metal flowed from central to around in the extrusion pressure, and the central protruded and bottom platforms were formed. In the second stage, the strain distributions in the two kind of forming processes had a great of differences. Effective strain of the claw root in thixo-forging reached 2.0, and the most of semi-solid metal except outermost layer were in the big strain zone. Effective strain of the claw root in forging reached only 1.1, and most of metal had smaller effective strain, which resulted in material flowing difficulty. In the last stage of metal forming, semi-solid material, due to its prior good strain distribution, could fill up claw easily, and the effective strain in the claw root reached 3.0, and the stress decreased to 30.8MPa. Whereas, effective strain in forging was smaller than that in thixo-forging, and its maximum effective strain in the claw root was only 1.91, and the stress reached 92.4MPa. Therefore, forging was more difficult in filling cavity than thixo-forging. That coincides with the experimental results.

Fig.11 showed the traditional forging and thixo-forging workpieces of magnesium alloy. The thixo-forging had better fill effect and surface finish quality than traditional forging, which could achieve near-end deforming with high workpiece quality. The maximum load was 0.35MN in traditional forging, and 0.24 MN in thixo-forging, which showed that the deforming force of semi-solid material was one third of that of traditional material in same conditions. The reason was that the branched grains formed continuous net framework structure in traditional forging. It had better support stress ability, higher deforming resistance and worse filling effect. In thixo-forging, the deformation force was required mainly to overcome particle sliding and particle plastic deformation, in which the sliding between solid particles and plastic deformation of solid particles mechanisms were dominant. The deformation resistance decreased obviously with deformation temperature increasing.

Fig. 9. Effective strain distribution of wrought magnesium alloy in thixo-forging process

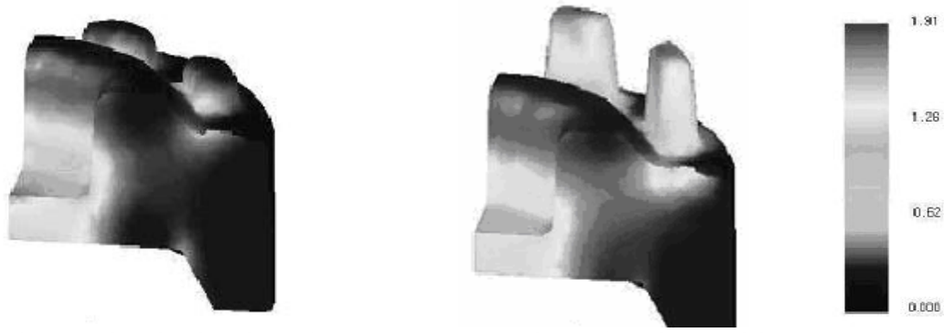

Fig. 10. Effective strain distribution of wrought magnesium alloy in traditional forging process

(a) Traditional forging workpiece (b) Thixo-forging workpiece

Fig. 11. Traditional forging and thixo-forging workpieces of wrought magnesium alloy

4.2 Finite element analysis of thixo- extrusion

The same simulated parameters were used to analyze the differences of mechanics properties, flow rule and temperature between traditional extrusion and thixo-extrusion processes. The extrusion set-up was shown in Fig.12. The materials were normal and semi-solid AZ61 wrought magnesium alloy respectively. Environment temperature was 20^{o}C, the warm-up temperature of die was 300^{o}C. The friction model was constant shearing stress model, whose friction factor was 0.65. Extrusion ratio was 4. Extrusion speeds were 100mm/s and 200mm/min respectively.

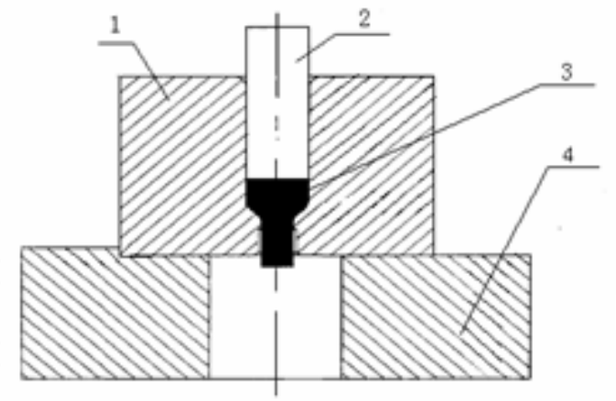

Fig. 12. Extrusion set-up (1.die 2.punch 3.billet 4.base seat)

Fig.13 and Fig.14 gave the effective strain distributions simulated results in extrusion and thixo-extrusion processes respectively. The strain distributions had few differences between extrusion and thixo-extrusion processes.

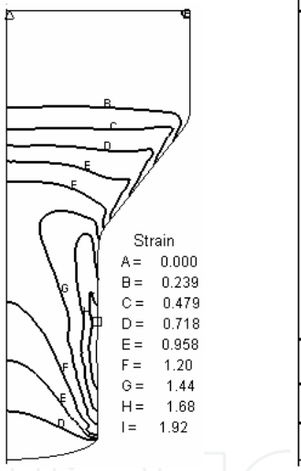

(a) step 18

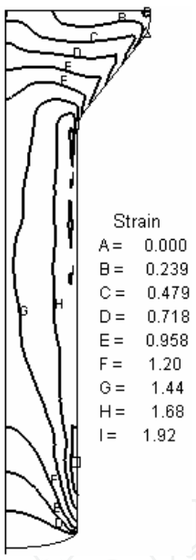

(b) step30

Fig. 13. Effective strain distributions in extrusion

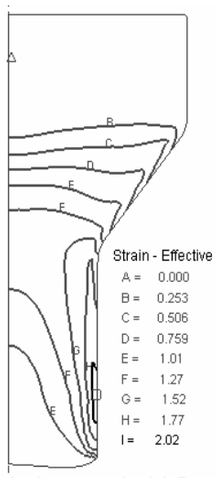

(a) step 18

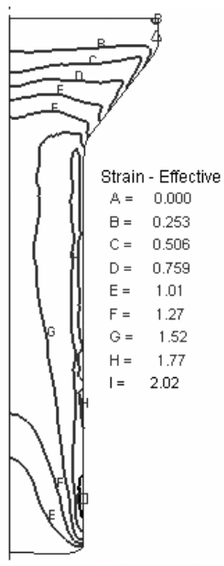

(b) step30

Fig. 14. Effective strain distributions in thixo-extrusion

Fig.15 showed the effective stress distributions before finished in extrusion and thixo-extrusion processes. From Fig.4a we could know that effective stress distribution existed unevenly in extrusion process, whose value was so big (100MPa) that the residual stress could be resulted in workpiece. That needed to add another working procedure for treating. The effective stress distribution in thixo-extrusion process was uniform and its value was small (30MPa), which was contributed from the excellent fluidity of semi-solid metal.

Distribution of temperature influenced the stress distribution of workpiece, which affected the local deformation resistance, and also influenced the distribution of strain and deformation fluidity. Fig.16 showed the temperature distributions in both extrusion and

thixo-extrusion processes. It could be gained that the temperature grads in extrusion process was larger than that in thixo-extrusion process, the former distribution was worse than the latter.

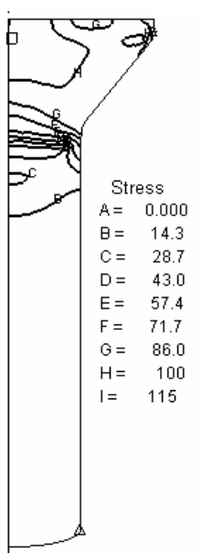

(a) extrusion

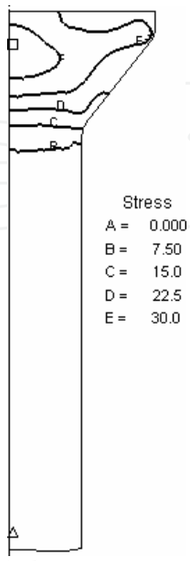

(b) thixo-extrusion

Fig. 15. Effective stress distributions

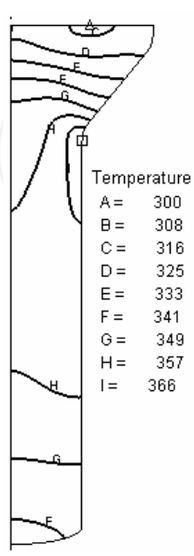

(a) extrusion

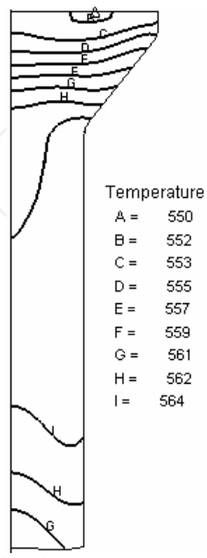

(b) thixo-extrusion

Fig. 16. Temperature distributions

The load-stroke curves between thixo-extrusion and conventional extrusion processes were shown in Fig.17(a) and Fig.17(b), in which the real line stood for extrusion speed 100mm/min and the broken line stood for extrusion speed 200mm/min. The deformation resistance in thixo-extrusion process was about 1/3 less than that in conventional extrusion process. The deformation resistance in conventional extrusion process was higher because a conventional dendritic structure formed the continuous mesh skeleton and the withstanding stress ability was stronger. The deformation resistance in thixo-extrusion process was lower, which was resulted from overcoming the grains' gliding and plastic deformation, because the liquid phase existed. The liquid phase increased with the temperature increasing, its resistance descended largely. Fig.17 (b) showed the thixo-extrusion load-stroke curves with different velocities and temperatures. The deformation resistance decreased with the increasing of temperature at the same velocity, in which the decreasing trend was obvious at the higher temperature. This reason was that the liquid membrane in the grain boundary was thicker and the grain' shape was close to spherical, made the grain turning and gliding more easy. The deformation resistance increased with the increasing of velocity at the same temperature. The maximum load in conventional extrusion process was 75KN at 300°C, which was 4 times larger than that in thixo-extrusion process. Simulation results were good agreement with experimental ones.

Fig.18 showed the samples resulted in thixo-extrusion process at different temperatures (590°C, 580°C, 570°C, 550°C, 530°C), in which the sample's surface was perfect with no crack when the temperature was lower than 570°C (Fig.18c-18e). The sample's surface had the micro crack above 580°C (Fig.18b), which become serious when the temperature reached 590°C (Fig.18a).

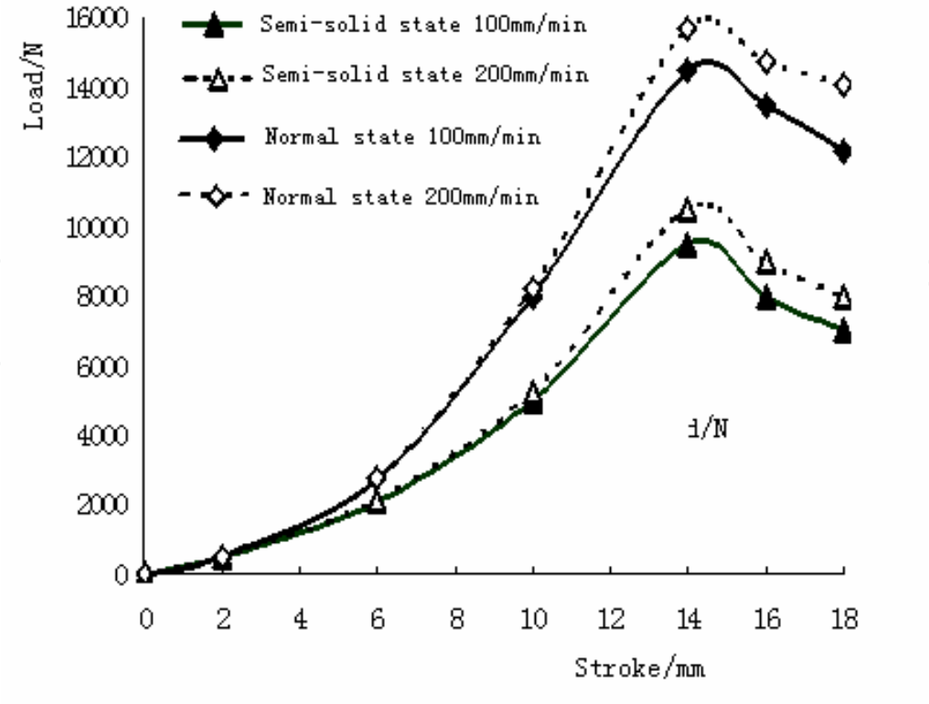

(a) Conventional extrusion and thixo-extrusion

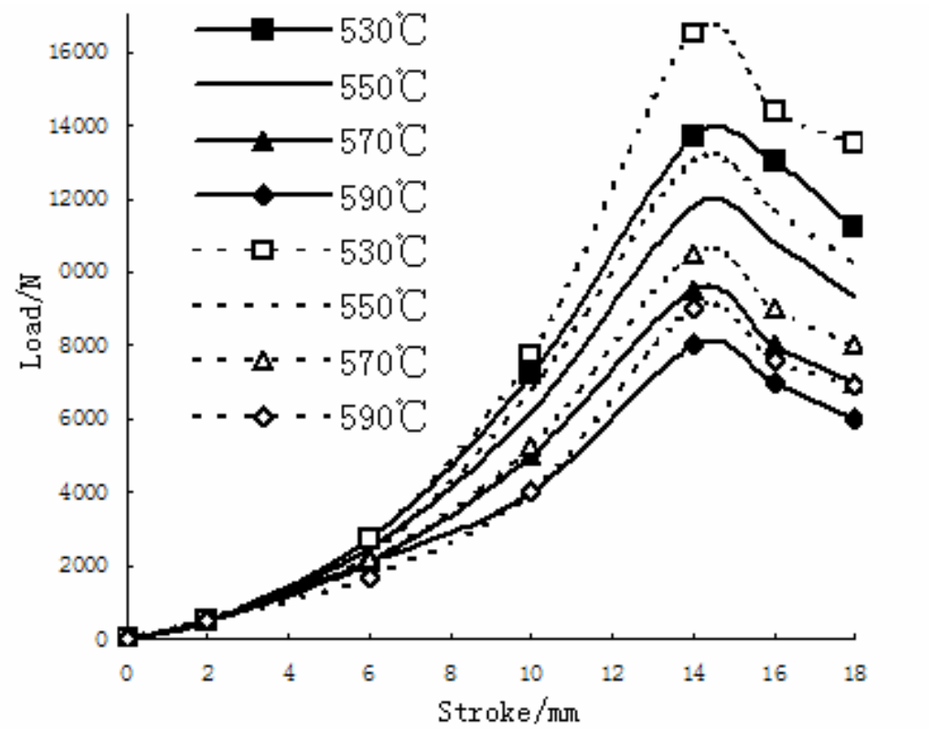

(b) Thixo-extrusion

Fig. 17. Load-stroke curves (speed: real line-100mm/min; broken line-200mm/min)

(a) 590°C

(b) 580°C

(c) 570°C

(d) 550°C

(e) 530°C

Fig. 18. Samples resulted in thixo-extrusion processes

5. Conclusion

Thixotropic deformation behaviours of semi-solid wrought magnesium alloy during compression process were obtained as follows: (1) The deformation force was required mainly to overcome particle sliding and particle plastic deformation in thixotropic compression process of high solid volume fraction for semi-solid AZ61 magnesium alloy, in which the sliding between solid particles and plastic deformation of solid particles mechanisms were dominant. (2) The deformation resistance decreased obviously with deformation temperature increasing under the same strain rate condition in thixotropic plastic compression processes for semi-solid AZ61 magnesium alloy.(3) The true stress peak value increased with the strain rate increasing under the same deformation temperature.(4) The deformation resistance of semi-solid AZ61 magnesium alloy was obviously smaller than one of conventional as-casted.

The proposed constitutive equation of semi-solid AZ61 was followed by

$$\sigma = \exp(25 - 11560 / T) \cdot \dot{\varepsilon}_Z^{0.026} \cdot \varepsilon_Z^{-0.09} \cdot (1 - \beta f_L)^{7.655}$$

The calculated results were good agreement with the experimental ones.

The flow stress models of AZ61 alloy for traditional forging/extrusion and thixoforming (thixo-forging and thixo-extrusion) were adopted to simulate the magnesium thixoforming process. The differences between the two forming processes were analyzed, and the following results have been obtained: (1) The deformation resistance in thixoforming was smaller than that in traditional forging/extrusion, in which the maximum load was about 1/3 less than that in traditional forging/extrusion. (2) The effective stress of workpiece in thixoforming was well distributed, whereas the stress concentration was liable to occur in traditional forging/extrusion, and in order to erase it more procedures should be supplemented. The effective strain of workpiece in thixoforming was distributed uniformly, its flow property and filling ability exceeded that in traditional forging/extrusion, so the complicated workpiece can be done once. (3) Simulation results were in good agreement with experimental ones. Numerical simulation can provide a help for the analysis of comparison between traditional forging/extrusion and thixoforming, and metal flow rule and plastic behavior accorded with practice can be obtained, which provide for the practice production as theory bases. (4) The semi-solid thixoforming technology has taken priority of the traditional processing.

6. Acknowledgement

This research was supported jointly by grant # 50465003 and # 50765005 from the National Natural Science Foundation of China, Innovative Group of Science and Technology of College of Jiangxi Province and the Jiangxi Province Education Commission Foundation.

7. References

Kang, C. G., Choi, J. S., Kim, K. H. (1999). The effect of strain rate on macroscopic behavior in the compression forming of semi-solid aluminum alloy. *Materials Processing Technology*, Vol.88, No.1-3: 159-168

Flemings, M. C. (1991). Behavior of metal alloy in the semi-solid state. *Metall Trans A*, Vol.22, No.5: 957-981

Yan, H., Xia, J. C. (2005). Theoretical analysis of plastic forming process for semi-solid material. *Materials Science Forum*, Vol.488-489, 389-392

Kang, C. G., Kang, B.S., Kim, J. I. (1998). An investigation of the mushy state forging process by the finite element method. *Mater. Pro. Tech.* Vol.80-81, 444-449.

Kiuchi, M., Yanagimtom, J., Yokobayashi, H. (2001). Flow stress, yield criterion and constitutive equation of mushy/semi -solid alloys, *Annals of the CIRP*, Vol. 50, 157-160.

Martin, C L., Favier, D., Suery, M. (1997). Viscoplastic behaviour of porous metallic materials saturated with liquid part I: Constitutive equations. *Int. J Plast.*, Vol.13, No.3, 215-235.

Yan, H., Zhou, B. F. (2006). Thixotrpic deformation behavior of semi-solid AZ61 magnesium alloy during compression process, *Materials Science and Engineering B*, Vol.132, No.1-2, 179-182.

Yan, H., Zhou, B. F. (2006). Constitutive model of thixotropic plastic forming for semi-solid AZ61 magnesium alloy. *Solid State Phenomena,* Vol.116-117, 577-682.

Tims, M. L., Xu, J., Nickodemus, G. (1996). Numerical simulation on thixoforming of wrought magnesium alloy. *Proceedings of Fourth International conference on Semi-solid Processing of Alloys and composites*, 120-124, UK, Sheffield.

Lipinski, D. M., Flender, E. (1998). Numerical simulation of flow and heat phenomena for semi-solid processing of complex casting, *Proceedings of the Fifth International Conference on Semi-solid Processing of Alloys and composites*, 273-277, USA, Colorado.

Yan, H., Zhang, F. Y. (2005). Structure evolution of AZ61 magnesium alloy in SIMA process. *Transactions of Nonferrous Metals Society of China,* Vol.15, No.3, 560-564.

Yan, H., Zhang, F. Y. (2006). Microstructural evolution of semi-solid AZ61 magnesium alloy during reheating process. *Solid State Phenomena,* Vol.116-117, 275-278.

Yan, H., Zhou, B. F. (2008). Study on thixo-forging of AZ61 wrought magnesium alloy. *Solid State Phenomena,* Vol.141-143, 577-682

Zhou, H. T., Zeng, X. Q., Wang, Q. D. and Ding, W. J. (2004). A flow stress model for AZ61 magnesium alloy. *Acta Metallurgic Sinica,* Vol.17, No.2, 155-160.

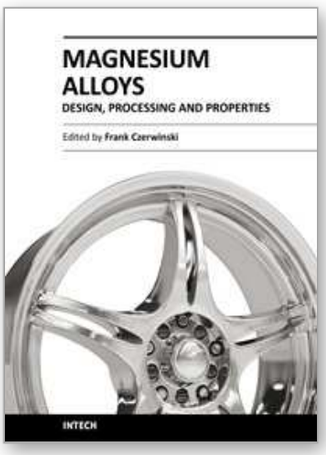

Magnesium Alloys - Design, Processing and Properties

Edited by Frank Czerwinski

ISBN 978-953-307-520-4
Hard cover, 526 pages
Publisher InTech
Published online 14, January, 2011
Published in print edition January, 2011

Scientists and engineers for decades searched to utilize magnesium, known of its low density, for light-weighting in many industrial sectors. This book provides a broad review of recent global developments in theory and practice of modern magnesium alloys. It covers fundamental aspects of alloy strengthening, recrystallization, details of microstructure and a unique role of grain refinement. The theory is linked with elements of alloy design and specific properties, including fatigue and creep resistance. Also technologies of alloy formation and processing, such as sheet rolling, semi-solid forming, welding and joining are considered. An opportunity of creation the metal matrix composite based on magnesium matrix is described along with carbon nanotubes as an effective reinforcement. A mixture of science and technology makes this book very useful for professionals from academia and industry.

INTECH
open science | open minds

InTech Europe
University Campus STeP Ri
Slavka Krautzeka 83/A
51000 Rijeka, Croatia
Phone: +385 (51) 770 447
Fax: +385 (51) 686 166
www.intechopen.com

InTech China
Unit 405, Office Block, Hotel Equatorial Shanghai
No.65, Yan An Road (West), Shanghai, 200040, China
中国上海市延安西路65号上海国际贵都大饭店办公楼405单元
Phone: +86-21-62489820
Fax: +86-21-62489821

IntechOpen